Zadorozhniuk *et al. Fire Ecology* (2026) 22:28
https://doi.org/10.1186/s42408-026-00454-y

Fire Ecology

RESEARCH

Open Access

Tree trunks do not bias estimates of surface fuels by aerial lidar in southern Sweden

Roman M. Zadorozhniuk[1*], Maksym Matsala[2], Olga T. Wepryk[2] and Igor Drobyshev[2]

Abstract

Background Surface and ladder fuels play a significant role in controlling fire behavior, and their estimation is critical for fire modeling and management. Although airborne laser scanning (ALS) provides cost-effective, spatially explicit data on forest 3D structure, its utility for surface fuel estimation remains uncertain due to canopy occlusion and the presence of tree trunk points. We assessed the impact of tree trunk point filtering (TPF) on model performance for estimating surface fuel loads in strata within a vertical gradient of 0.0–2.0 m, which includes litter, herbaceous, and shrub layers. We used high-density ALS data (~ 2500 points m^{-2}) from boreo-nemoral mixed forests in southern Sweden. We compared the performance of 438 LiDAR (lidar) metrics in characterizing surface fuels using parametric (linear and non-linear) and nonparametric (random forest — RF) regressions.

Results There was no significant impact of TPF when comparing lidar-derived metric distributions and model performance under filter types, although a minor improvement was observed in the 0.5–2.0-m stratum. The performance of surface fuel strata modeling was the highest for the litter layer depth ($R^2 = 0.39$) and moderate for the herbaceous layer and branch biomass ($R^2 = 0.26$–0.28). The linear regression model consistently outperformed the RF model and showed slightly better performance than the nonlinear regression. We obtained a negligible positive impact of TPF ($\Delta R^2 = 0.02$) on predicting the litter layer depth utilizing the parametric regression approaches. Intensity-based metrics calculated using a minimum 5-m buffer radius were instrumental in modeling fuel layers within the 0.0–0.5-m stratum.

Conclusions Removing tree trunk points did not affect the representation of surface fuels in airborne lidar data. We suggest, however, that the correct classification of ground and no-ground points and detection of objects such as boulders and deadwood can have a major effect on the adequate prediction of surface fuels.

Keywords Fuel loads, Trunk points filtering, Ladder fuels, Boreal forests, Aerial lidar, Prescribed burning

Resumen

Antecedentes Los combustibles superficiales y las escaleras de combustible juegan un rol significativo en el control del comportamiento del fuego, y su estimación es crítica para el modelado y el manejo del fuego. Aunque la técnica de escaneo láser aerotransportado (*airborne laser scanning,* ALS de ahora en más), provee datos espacialmente explícitos y rentables para caracterizar la estructura forestal en 3D, su utilidad para la estimación de combustibles superficiales sigue siendo incierta debido a la oclusión que presentan los doseles y la presencia de los troncos de los árboles. Determinamos el impacto del filtrado de puntos que representan troncos de árboles (*Trunk Point Filtering,* TPF) sobre la performance del modelo para estimar la carga de combustible superficial en estratos con un gradiente

*Correspondence:
Roman M. Zadorozhniuk
zadorozhniuk@nubip.edu.ua
Full list of author information is available at the end of the article

vertical de 0,0 a 2,0 m, incluyendo los estratos de broza, hierbas y arbustos. Usamos datos de ALS de alta densidad (~ 2.500 puntos por m^2) de bosques mixtos boreales del sur de Suecia. Comparamos la performance de las métricas del LIDAR 438 para caracterizar los combustibles superficiales usando regresiones paramétricas lineares y no lineares, y no paramétricas (Bosques al Azar, o RF).

Resultados No encontramos un impacto significativo de TPF cuando comparamos las distribuciones de métricas derivadas de LIDAR y la performance del modelo bajo tipos de filtros, aunque un pequeño mejoramiento fue observado en el estrato entre 0,5 y 2,0 m. La performance del modelo que consideraba los combustibles superficiales fue mayor para el estrato que marcaba la profundidad de la broza ($R^2 = 0{,}39$), y moderado para el estrato herbáceo y el de las ramas ($R^2 = 0{,}26–0{,}28$). El modelo de regresión linear consistentemente superó al modelo de RF y mostró una mayor performance que el de regresión no linear. Obtuvimos un impacto positivo insignificante en TPF ($\Delta^{R2} = 0{,}02$) en predecir la profundidad del estrato de la broza utilizando las aproximaciones de regresión paramétricas. Las métricas basadas en intensidad calculadas usando un radio de buffer mínimo de 5 m fue instrumental para el modelado de estratos de combustibles dentro de los 0,0 y 0,5 m de esos estratos.

Conclusiones La remoción de los puntos de los troncos no afectó la representación de los combustibles superficiales en los datos obtenidos mediante la técnica del escaneo laser aerotransportado (ALS). Sugerimos, por supuesto, que una correcta clasificación de puntos en el suelo y a detección de objetos como rocas y troncos muertos puede tener un efecto mayor en la adecuada predicción de los combustibles superficiales.

Background

Wildfires are a natural disturbance agent whose impact in the boreal region has been increasing over the last decades (Ellis et al. 2022; Iglesias et al. 2022; Jones et al. 2022). Uncontrolled wildfires lead to economic losses, profound impacts on ecosystem functioning and biogeochemical cycles, and can cause the transition of forests into non-forested ecosystems (Stephens et al. 2014; Seidl and Turner 2022; Seidl et al. 2024). The implementation of fire management systems helps mitigate these risks through fuel load manipulation and fire behavior modeling (Keane 2013). Fire behavior models require several key input parameters, including fuel characteristics, weather conditions, and topography (Cardil et al. 2021). At the landscape level, fuels are typically characterized as static categorical types within the corresponding landscape, while effective decision-making relies on situational awareness supplemented by high spatiotemporal resolution data (Myroniuk et al. 2023). Because forest fuels are one of the fundamental components within forest structure that control fire risk and fire behavior (Prichard et al. 2020; Wepryk et al. 2025), their accurate assessment is crucial for effective wildfire management (Barros et al. 2018; Lesmeister et al. 2019; North et al. 2022).

Historically, the most common technique for estimating fuel load was destructive measurement methods (Catchpole and Wheeler 1992). However, such in situ surveys of surface fuel load are labor-intensive, spatially limited, and impractical for frequent monitoring across large areas (Brown 1974; Lutes et al. 2006; Keane 2015; Lin et al. 2024). Traditional in situ surveys are based on plot- or transect-level measurements that provide spatially averaged estimates of surface fuel load values (Brown 1974; Lutes et al. 2006; Keane 2015) while failing to capture their fine-scale variability within forest stands (Sánchez-López et al. 2025). Despite their precision, traditional plot- and voxel-based (Hawley et al. 2018) assessments are too labor-intensive to provide efficient fuel data for large-scale fire behavior modeling (Keane 2013). Even within a single plot, components such as herbaceous biomass, litter depth, or shrub biomass can exhibit substantial heterogeneity driven by micro-topography, light availability, and canopy structure (Pelt and Franklin 2000). As a result, conventional fuel inventories often smooth this variability into generalized fuel descriptors that may not adequately represent local fuel conditions. Transitioning from traditional fuel assessments toward regularly updated fuel load maps using remote-sensing data (Gale et al. 2021; Sánchez-López et al. 2023; Bright et al. 2022) can improve our ability to model and manage fires.

Recent technological developments in the field of remote sensing have led to the characterization of three-dimensional (3D) forest structure using LiDAR (Light Identification, Detection and Ranging, further — lidar) (Cimdins et al. 2025; Wulder et al. 2022). To date, aerial laser scanning (ALS) has become one of the most widely used technologies for forest structure assessment, providing information at sub-meter resolution (Ross et al. 2024). The main advantage of ALS lies in its ability to penetrate through forest canopy, enabling a detailed structural characterization of forest stands and their fuel components across vertical strata. Numerous studies have demonstrated the effectiveness of ALS in quantifying fuels in the main canopy (Andersen et al. 2005;

Maltamo et al. 2020; Tenny et al. 2025), ladder fuels (Forbes et al. 2022), and surface fuel (Jarron et al. 2020; Stefanidou et al. 2020; Bright et al. 2022; Loudermilk et al. 2023; Labenski et al. 2023; Arkin et al. 2025).

Previous studies have demonstrated that ALS is particularly effective in capturing the vertical distribution of fuels (Viedma et al. 2024) and in predicting key forest canopy parameters such as canopy height, canopy base height, and canopy bulk density (Skowronski et al. 2011; Maltamo et al. 2020; Cameron et al. 2022), as well as estimating forest canopy consumption during fire events (McCarley et al. 2017). These metrics are critical inputs for fire behavior models, as they govern processes such as sustained crown fire spread. Importantly, canopy base height defines a crucial threshold for crown fire initiation (Hall and Burke 2006; Scott and Burgan 2005).

Meanwhile, surface fuels remain more challenging to be quantified by ALS, particularly under closed tree canopies (Gale et al. 2021; McCarley et al. 2024). This technical gap is crucial, as the ignition and propagation of the majority of wildland fires are driven by surface fuels, which consist of a diverse array of physically distinct fuel types within forested environments (Keane 2013; 2015). When the ability of ALS-derived metrics to accurately represent surface fuel variability remains uncertain, these surveys provide large-scale and cost-effective inventories of forest attributes without high point density (Gale et al. 2021; Labenski et al. 2023). While ALS-based models of surface fuel load may yield lower explanatory ability compared to terrestrial lidar scans or traditional surveys (Jakubowksi et al. 2013; Arkin et al. 2025), ALS enables spatially continuous fuel characterization over large areas, thereby shifting the focus from maximizing sample plot-level accuracy to capturing fuel variability across the landscape (Gale et al. 2021; Jakubowksi et al. 2013).

Terrestrial laser scanning (TLS), a ground-based form of lidar technology that acquires measurements from beneath the forest canopy, is another lidar-based method that can serve as an alternative to in situ forest measurements (Laino et al. 2024), even over-performing accuracy of conventional surface fuel surveys (Li et al. 2021). TLS describe fine-scale 3D forest structure utilizing high-density point clouds (Åkerblom and Kaitaniemi 2021). However, this approach forfeits spatial coverage that can be achieved (Calders et al. 2020; Xi et al. 2023). This technology provides a more detailed estimation of forest understory layers, which is limited to aerial systems due to occlusion by tree canopies (Rowell et al. 2020; Arkin et al. 2025). TLS data in forest understory can be collected using static scanning (Wallace et al. 2016) and various mobile systems (Loudermilk et al. 2012; Ryding et al. 2015; Bauwens et al. 2016; Hyyppä et al. 2020; Balenović et al. 2021; Adhikari et al. 2023).

The filtration of a particular vegetation layer is a frequently employed approach to enhance the extraction of target structural information in lidar data processing (Arrizza et al. 2024). The assessment of leaf area index is one example where filtering out woody components is important (Woodgate et al. 2016; Zhu et al. 2020; Flynn et al. 2023). Removing canopy returns or their stratification is required for characterization of understory vegetation (Hamraz et al. 2017; Jarron et al. 2020; Du and Pang 2024) or vice versa — overstory layer estimation (Bouvier et al. 2017; Penner et al. 2024; Chen et al. 2025). Filtering may be required not only for the separation of canopy and understory layers but also for accurate tree trunk detection and diameter estimation, or assessment of deadwood on the ground layer (Heinaro et al. 2021) requires the filtering of foliage and noise (An and Froese 2023). Additional filtration techniques that may be employed for the evaluation of forest parameters include leaf-off laser scanning approaches (White et al., 2015; Maltamo et al. 2025) and leaf-wood separation (Arrizza et al. 2024; Chen et al. 2025).

In this study, we evaluated the impact of trunk point filtering (TPF) on the performance of surface fuel predictive models in mixed boreo-nemoral forests of southern Sweden. Although filtering is a commonly used approach in lidar data processing, the impact of applying these approaches on surface fuel load assessment has not been investigated. For instance, in areas dominated by shrubs or trees, points originating from standing tree trunks have the potential to contaminate the estimated strata points. This can significantly reduce the accuracy of models aimed at estimating ground or near-surface fuel. Such contamination results in points representing under canopy layers being a mixture of points from tree trunks, shrub layers, or herbaceous vegetation. Earlier research primarily addressed the detection of tree trunks in forests, which is now a relatively trivial task for forest measurement purposes (De Conto et al. 2017; Laino et al. 2024). Yet, there is a paucity of studies that have evaluated the impact of TPF that do not describe surface or ladder fuels, in part because ALS point densities often remain insufficient for accurate trunk detection. However, while such tasks are well suited for TLS data, in our study, we employed very high-density ALS acquired from low flight altitudes. The obtained point cloud density was ~ 2500 points m^{-2}, which was substantially higher than the ALS point densities (varying from 10 to 500 points m^{-2}) typically used for surface fuel assessment (McCarley et al. 2024; Stefanidou et al. 2020; Bright et al. 2022; Labenski et al. 2023; Arkin et al. 2025). We expected that such a high point density would reduce uncertainties in the representation of surface fuel structure, which is often poorly described in conventional ALS

datasets (e.g., herbaceous plants, litter). The second aim of utilizing such high point density ALS data was to accurately and automatically delineate points of tree trunks. We combined these data with small in situ sample plots of 1-m radius, where surface fuel load data in vertical strata up to 2.0 m was collected (litter, herbaceous, and shrublands layers). The aim of our study was therefore twofold: (i) To examine the potential of high-density ALS to predict surface fuel load in boreo-nemoral forests and (ii) to evaluate the effect of TPF on the predictive performance of these models.

Materials and methods

Site description

The study was conducted in three forests located in Kalmar province, southern Sweden. All sites, Högahyltan, Mjösjögöl, and Sandvik, were within the Allgunnen Nature Reserve (Fig. 1). The reserve lies in the boreo-nemoral vegetation zone (Sjörs 1963). The regional mean annual temperature is 8.5 °C, and the mean annual precipitation is 486 mm (SMHI 2025).

Sandvik is an uneven-aged stand dominated by 150-year-old Scots pine (*Pinus sylvestris* L.), which forms the upper canopy. The sub-canopy consists of pedunculate oak (*Quercus robur* L.) and aspen (*Populus tremula* L.), with small, irregular clusters of Norway spruce (*Picea abies* (L.) H. Karst.). The forest ground layer is composed primarily of mosses (*Hylocomium splendens* Schimp. and *Pleurozium schreberi* Mitt.), bilberry (*Vaccinium myrtillus* L.), lingonberry (*Vaccinium vitis-idaea* L.), and varying proportions of oak litter, with occasional spruce branches, star reindeer lichen (*Cladonia stellaris* Opiz), and heather (*Calluna vulgaris* L.). A prescribed burn was carried out in 2023 with the objectives of reducing 5–15% of the pine population and at least 80% of the spruce to increase canopy openness and ground-level light availability (Länsstyrelsen i Kalmar län Bränningsplan Allgunnen Sandvik, 2023, Kalmar, Sweden, internal unpublished report).

Högahyltan is a 30-year-old mixed stand of Scots pine, pedunculate oak, and silver birch (*Betula pendula* Roth). The ground vegetation is dominated by mosses, bilberry,

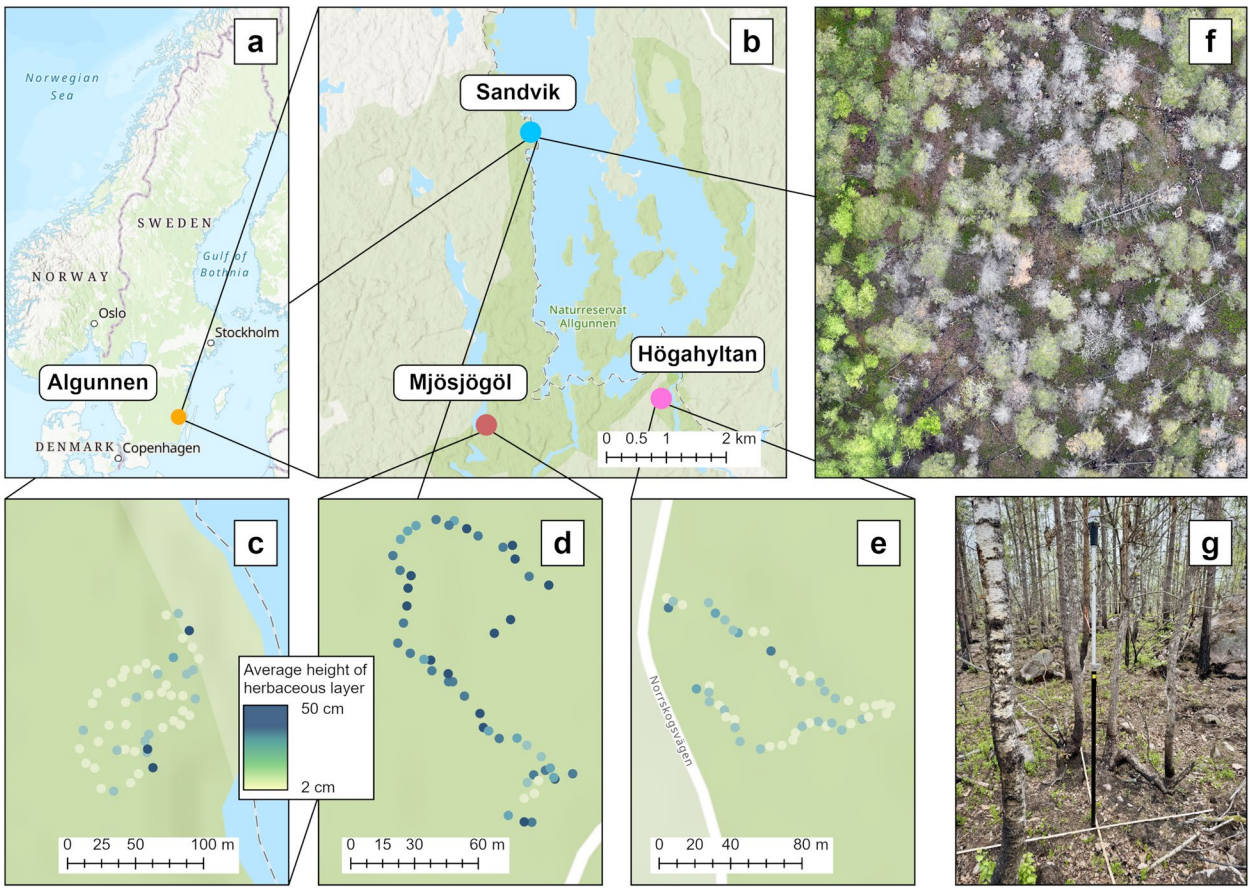

Fig. 1 Sample plots representation. **a** Location of Allgunnen Natural Reserve in Sweden. **b** Locations of study sites in Allgunnen Natural Reserve. **c** Sample plots in Sandvik site. **d** Plots in Mjösjögöl site. **e** Plots in Högahyltan site. **f** Example of burned boreo-nemoral landscape in Sandvik site, aerial view from drone. **g** Example of sample plot with Emlid Reach RX network rover at plot center

lingonberry, and oak litter. In 2024, a prescribed burn was implemented with the goal of opening the canopy, promoting deadwood formation, and suppressing spruce regeneration (Länsstyrelsen i Kalmar län: Bränningsplan Allgunnen Högahyltan, 2024, Kalmar, Sweden, internal unpublished report).

Mjösjögöl is characterized by a mature overstory of Scots pine (150 years old), with a secondary layer of pedunculate oak and aspen aged 50–60 years. Scattered clusters of Norway spruce occur throughout the stand. The forest ground layer consists primarily of mosses and berry species, with occasional star reindeer lichen (Länsstyrelsen i Kalmar län: Bränningsplan Allgunnen Mjösjögöl 2025, Kalmar, Sweden, internal unpublished report).

Field data acquisition and description

We established 150 circular sample plots (1-m radius) within our study forests, with 50 plots in each site. We georeferenced plot centers using Emlid Reach RX network rover with Real-Time Kinematics (RTK) module (horizontal accuracy ~ 2 cm). We sampled plots along predefined tracks with a minimum distance between sample plots of ~ 3 m. The location of sample plots was chosen subjectively, aiming to represent the heterogeneity of the study areas instead of following a purely random design. This approach was applied consistently across all sites. Because two of the three sites had experienced prescribed burning, fuel conditions were highly heterogeneous, and random sampling could have resulted in an overrepresentation of plots lacking any understory vegetation. The chosen approach allowed us to evenly capture the observed variability in surface fuel structure and composition.

We developed a specific fuel assessment protocol, which included characterization of fuel strata along vertical gradient in the forest. First, we measured litter depth, visually estimated the horizontal cover of the herbaceous layer as a percentage, and measured the average height of that layer (≤ 0.5 m). Herbaceous layer height was measured at five randomly selected points within each plot, and the mean value was used in the analyses. Second, we counted all tree and shrub branches within the plot and vertical stratum of 0.5–2.0-m height if their diameter (in the middle of length) was above 0.1 cm. We measured the vitality (dead or alive) and diameters on 0.5 height of shrubs within sample plot. We also recorded the average length of these branches. We recorded the lying deadwood within the plot (if the diameter was above 5 cm) and the ratio of branches in the 2.0–5.0-m vertical strata, but this information was not used for fitting models in this study. Finally, we measured diameter at breast height of all standing trees within the plot and captured the vitality. Consequently, the density of herb stratum and the volume of shrubs and brunches were converted into biomass using biomass expansion factors (Jalkanen et al. 2005; Lutes et al. 2006).

Out of a total of 150 sample plots, 71 exhibited the presence of at least one tree. The diameter of these tree trunks, measured at breast height, ranged from 5 to 36 cm with an average of 13 cm (Table 1).

ALS data acquisition

Lidar data was collected by using a DJI Matrice 350 drone equipped with an RTK module. The receiving sensor detected up to five returns with each laser beam emitted. We flew at low altitudes (35 m above ground) with horizontal and vertical overlaps of 80%. This allowed us to collect lidar data with point densities ranging from 2354 to 2913 points m^{-2} and pulse densities from 1444 to 1858 pulses m^{-2}. All data were stored in LAS format (version 1.2, point format 3) and referenced to the SWEREF99 TM coordinate system.

ALS data preparation

Statistical analysis was conducted in R (R Core Team 2025). Even though the sample plots had an in situ radius of 1.0 m, ROI (region of interest) were clipped with a 10-m radius buffer using the LidR package (Roussel et al. 2020). This increased radius was necessary to perform the optimization of parameters for tree trunk point classification (Fig. 2). Prior to ROI extraction, the full ALS point cloud covering the study forests was preprocessed. Ground points had been classified during the generation of the initial LAS files in DJI Terra (DJI, Shenzhen,

Table 1 Descriptive statistics of field data

Variable	No. of observation	Measurement unit	Mean	Standard deviation	Min	Max	Median	The interquartile range
Herbaceous layer	150	$t{\cdot}ha^{-2}$	111.21	144.01	2.55	755.16	40.25	147.77
Litter depth	100	cm	6.31	4.56	0.10	20.50	5.45	6.14
Branches	150	$t{\cdot}ha^{-2}$	5.75	12.56	0.00	75.00	0.00	5.82
Branches and dead shrubs	150	$t{\cdot}ha^{-2}$	6.11	12.65	0.00	75.00	0.10	7.01

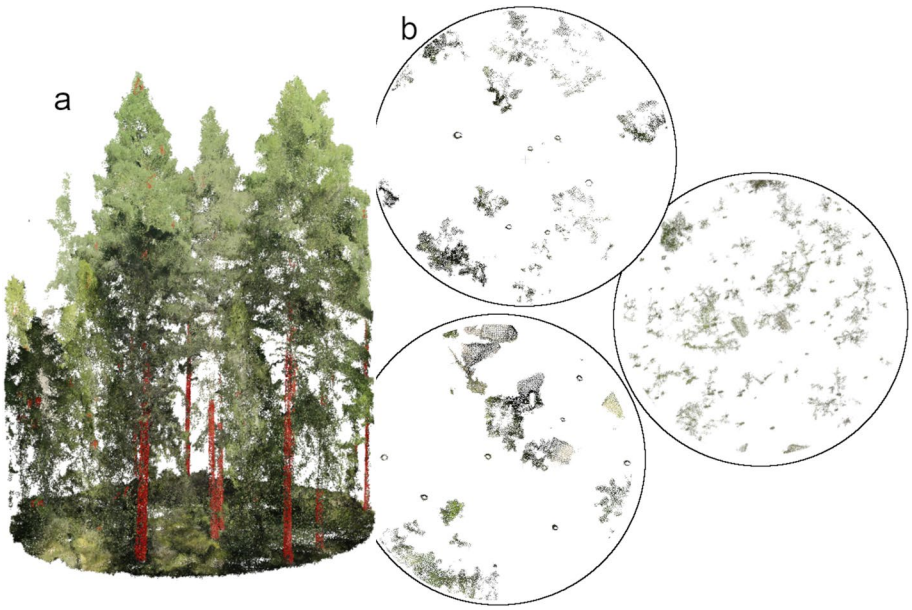

Fig. 2 Example of visual representation of a clipped point cloud in ROI (10-m radius) for a sample plot. **a** RGB-colored ALS point cloud with classified tree trunk points (red colored). **b** Cross sections of the ROI clipped at 0.5-m height and 1-m width, which represent tree trunks and understory vegetation

China), after which we utilized lidR package for point cloud processing, where we created a digital terrain model (DTM) with a spatial resolution of 0.2 m, and normalized point clouds.

We performed tree trunk filtering by processing each ROI using the TreeLS package in R (De Conto et al. 2017). In this study, we compared three data treatments: "no-filtered" point clouds, a standard "semi-filtered" approach, and an enhanced "upsize-filtered" approach. The "semi-filtered" approach required the filtration of points classified as tree trunks, which was conducted using the TreeLS package. At this step, we calculated eigen decomposition metrics using *knn* ($k=20$) method. As the semi-filtered approach did not fully capture tree trunk points, the "upsize-filtered" method was implemented to ensure consistent removal of trunk-related returns (Fig. 3). We extracted all points within a 0.25-m voxel (0.3 m in height) centered around each previously classified tree trunk point. The vertical extent of the upsize filter was limited from the maximum height of the initial fuel stratum down to the canopy base height (CBH), which allowed us to isolate trunk-related returns within the relevant vegetation layer.

Extraction of lidar-derived metrics

For the modeling of each surface fuel component, we calculated a total of 400 + lidar-derived metrics, which were obtained across six groups: based on height distributions, point density, geometry, intensity (in near-infrared part of electromagnetic spectrum), voxel based, and the estimation of leaf area density (LAD). We utilized the LidR package as the environment (Roussel et al. 2020) for lidar-derived metrics calculation within sample plots, additionally applying rLiDAR and leafR during LAD calculation. The estimated variables were grouped by type and fuel load strata (Labenski et al. 2023). All calculated variables were used to predict the following fuel strata: 0.0–0.5 m (corresponding herbaceous and litter layers) and 0.5–2.0 m (corresponding shrub layer). We calculated lidar-derived metrics primarily within the corresponding vertical strata. However, we experimentally adjusted the vertical boundaries of the strata—either narrowed or expanded (Table 2)—to explore their relationships with surface fuel properties. To account for the potential influence of overlying vegetation on lidar signal intensity and to capture their relation with independent variables, we computed intensity-based metrics using a conventional sample plot size, as well as vertically and horizontally extended buffers (up to 5 m).

Statistical analyses

Prior to development of models, we selected independent variables using a sequential procedure. First, we evaluated the correlation between response variables and all candidate variables within the corresponding fuel strata using Pearson correlation analysis. At this stage, we excluded independent variables that had no statistically significant correlation ($p \geq 0.1$). Second, from the

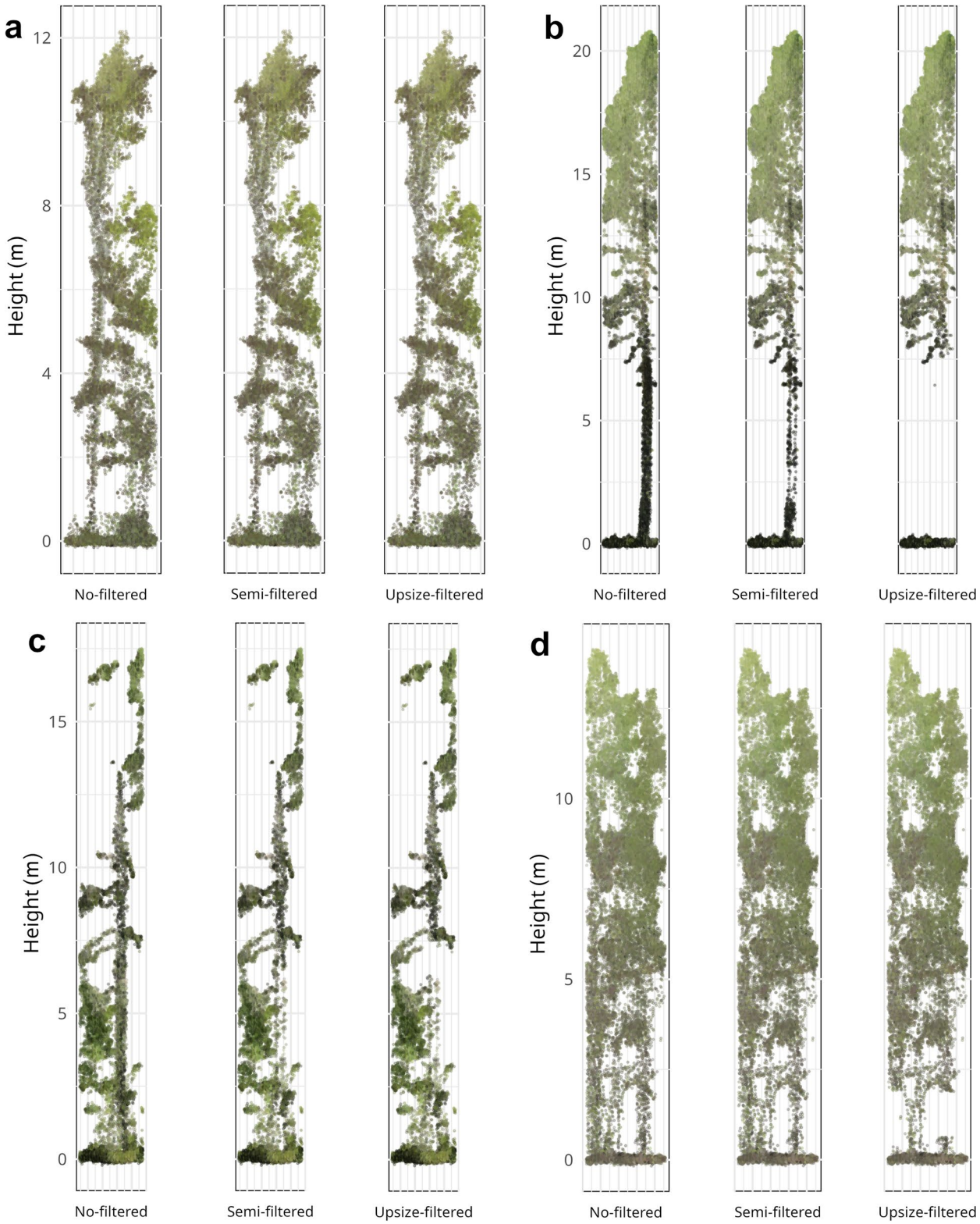

Fig. 3 The vertical profiles of the point cloud within sample plots (1-m radius). **a** Lack of extraction, **b** extraction, and **c**, **d** partial extraction

Table 2 Description of lidar-derived variables

Metrics group	Acronym[a]	Description	Vertical strata limits	No. of variables
Height	zmax, zmean, zsd_st, zskew, zkurt, zentropy, pzabovezmean, pzabove2, zq_(5, 10, … 95), Q (99, 95, … 10), N_points Zpcum (1, 2, … 9)	Maximum, mean, standard deviation, skewness, and kurtosis of points within stratum and stand Entropy, proportion of points above the mean height, proportion of points above the 2-m height, height quantiles (5–95% range with 5% step) within stand Height quantiles (10, 25, 50, 75, 90, 95, 99) and the number of points calculated within stratum Cumulative height distribution metrics, i.e., showing what percentage of points were below a certain threshold of the maximum height (90, 80, … 10%) calculated within stratum and stand	0.0–0.5, 0.0–2.0, 0.0–max	80
Density	P_below, P_column	The proportion of the number of points within strata to the points within strata and below strata together The proportion of the number of points within strata to the total number of points in the stand's vertical column	0.1–0.5, 0.25–0.5, 1.0–2.0, 0.5–2.0	8
	V1	Proportion of first return points relative to all points in vertical column	0.0–max	1
Geometry	EL, EM, ES curv, lin, plan, shp, ani, hor	Eigen_largest, eigen_medium, eigen_smallest, curvature, linearity, planarity, sphericity, anisotropy, horizontality were calculated separately included and excluded ground points (ngr)	0.0–0.5, 0.1–0.5, 0.0–0.3, 0.05–0.3, 0.25–0.5, 1.0–2.0, 0.5–2.0, 2.0–5.0	144
Intensity	_I_	Distribution of intensity variable (mean, variation, standard deviation, coefficient of variation, skewness), estimated separately within sample plot and with 2- or 5-m buffers (statistics were calculated separately for the first returns only and for all returns)	0.01–0.5, 0.5–2, 1.0–2.0, 2.0–5.0, 0.0–5.0	150
Voxel	_V_	Statistics are calculated for each stratum separately with 10-cm voxel resolution: • The number of non-empty voxels per stratum • The mean number of points per voxel • The standard deviation per voxel • The coefficient of variation per voxel • The proportion of voxels with data to the total number of voxels (voxel ratio)	−0.1–0.5, 0.1–0.5, 0.25–0.5, 0.0–0.5, 0.1–0.4, 0.0–0.4, − 0.1–0.4, 0.0–0.3, 1.0–2.0, 0.5–2.0	50
LAD	GS	Gini-Simpson (GS) index of foliage structural diversity (Valbuena et al. 2012)	0.0–5.0	1
	gini	The value of the inequality measure of Gini	0.0–max	1
	LAD	Mean value of LAD within stratum calculated using rLiDAR package	0.0–5.0, 0.5–2.0	2
	lai	Lai values within stratum calculated using leafR package (Almeida et al. 2019)	0.5–2.0	1

[a] The first number after the symbol is the lower height, and the second is the upper height of vertical stratum

subset of statistically significant variables, we selected the highest correlated variables within each predefined ALS-derived metric group (Table 2). This step aimed to retain representative metrics while limiting redundancy and resulted in approximately 10–15 candidate predictors per fuel type. Finally, we conducted pairwise Pearson correlation in order to remove multicollinearity among the selected independent variables. When strong correlations between independent variables were detected ($r > 0.8$), only one variable from each correlated pair was

retained. The resulting set of predictors was applied consistently across all model types.

We performed Student's *t*-test (Student 1908) to analyze the differences in lidar-derived metric distributions among the various tree trunk filtering approaches. Prior to testing, the normality of the data distribution was assessed using the Shapiro–Wilk test (Shapiro and Wilk 1965).

We applied three regression approaches to model surface fuels: Random forest (RF), linear regression (LR), and nonlinear regression (NLS) using the nonlinear least squares method. To address the fact that the data distribution was right-skewed, we used a square root transformation of the dependent variable distributions representing herbaceous and litter layers. We employed this transformation of dependent variables across all modeling approaches, while independent variables were transformed during utilization only with the NLS regression approach. Leave-one-out cross-validation (LOOCV) was used to validate the model performance (Stone 1974), as we did not have systematic, unbiased sampling design.

We evaluated model performance using the root-mean-squared error (RMSE), relative RMSE ($RMSE_{\%}$), bias, and relative bias ($bias_{\%}$):

$$R^2 = 1 - \frac{\sum_{i=1}^{n}(y_i - \hat{y}_i)^2}{\sum_{i=1}^{n}(y_i - \bar{y})^2} \quad (1)$$

$$RMSE = \sqrt{\frac{\sum_{i=1}^{n}(\hat{y}_i - y_i)^2}{n}} \quad (2)$$

$$RMSE_{\%} = \frac{RMSE}{\bar{y}} \times 100 \quad (3)$$

$$bias = \frac{\sum_{i=1}^{n}(\hat{y}_i - y_i)}{n} \quad (4)$$

$$bias_{\%} = \frac{100 \times Bias}{\bar{y}} \quad (5)$$

where $\hat{y}$ is the predicted value, y_i is the observed value, and $\bar{y}$ is the mean of the observed values. The same set of independent variables was used in all regressions.

Results

Variable selection

Some groups of metrics were completely excluded from modeling specific fuel stratum (Table 2, Fig. 4). For modeling the 0.5–2.0-m fuel layer, three groups of metrics were selected for the modeling: height-, geometry-, and voxel-based metrics. Density-based metrics were retained in the models only for the 0.0–0.5-m stratum. Voxel-based metrics showed weak relationships within the 0.0–0.5-m stratum while being important predictors for the 0.5–2.0-m stratum. Height-based metrics consistently contributed across all layers, with cumulative metrics being especially relevant. Geometry metrics also played a significant role across all dependent strata. In contrast, LAD metrics were not included in the final models because they exhibited multicollinearity with other selected predictors and, generally, showed weaker relationships with fuel load than voxel-based metrics, especially within the 0.5–2.0-m stratum.

Intensity metrics (calculated at 5-m buffer) were relevant exclusively for the 0.0–0.5-m stratum. Using buffers with 1- or 2-m radii decreased the correlation between intensity metrics and the response variables. However, the choice between using first returns and all returns did not impact this relationship.

Impact of filtering tree trunk points out

TPF significantly influenced lidar-derived metrics for the strata beyond 0.5 m. There were no significant differences ($p < 0.05$) in the distributions of lidar point counts within the corresponding strata (Fig. 5). In 0.0–0.5-m stratum, we observed a minor change in point density. That is, the high density of herbaceous points representing this vegetation reduced the relative contribution of tree trunk points. In the 0.5–2.0-m stratum, the lidar data frequently contained tree trunk points, making the impact of filtering much more evident but still no significant ($p = 0.41$, Fig. 5). Consequently, the impact of filtering on lidar-derived variable distributions was less pronounced for metrics derived from the 0.0–0.5-m stratum (corresponding herbaceous and litter layers). TPF had less impact on variables' distribution in intensity- and geometry-based groups (Table 2, Fig. 6). The most substantial changes were observed in the cumulative height metrics, as well as in the voxel occupation ratio within the 0.5–2.0-m layer (Fig. 6). Filtering affected the voxel occupation ratio at their value ranges up to 0.1 (Fig. S1), but this effect disappeared once the ratio exceeded 0.1 (bulk density > 10%).

Although the results of paired *t*-test analysis of variance indicate a predominantly statistically significant effect of filtering on the differences between no-filtered and semi-filtered variables (Fig. S1, Fig. S2), no statistically significant difference was observed between the no-filtered and upsize-filtered data.

Model performance

For all fuel components, R^2 did not exceed the value of 0.4 in leave-one-out cross-validation (Fig. 7). LR

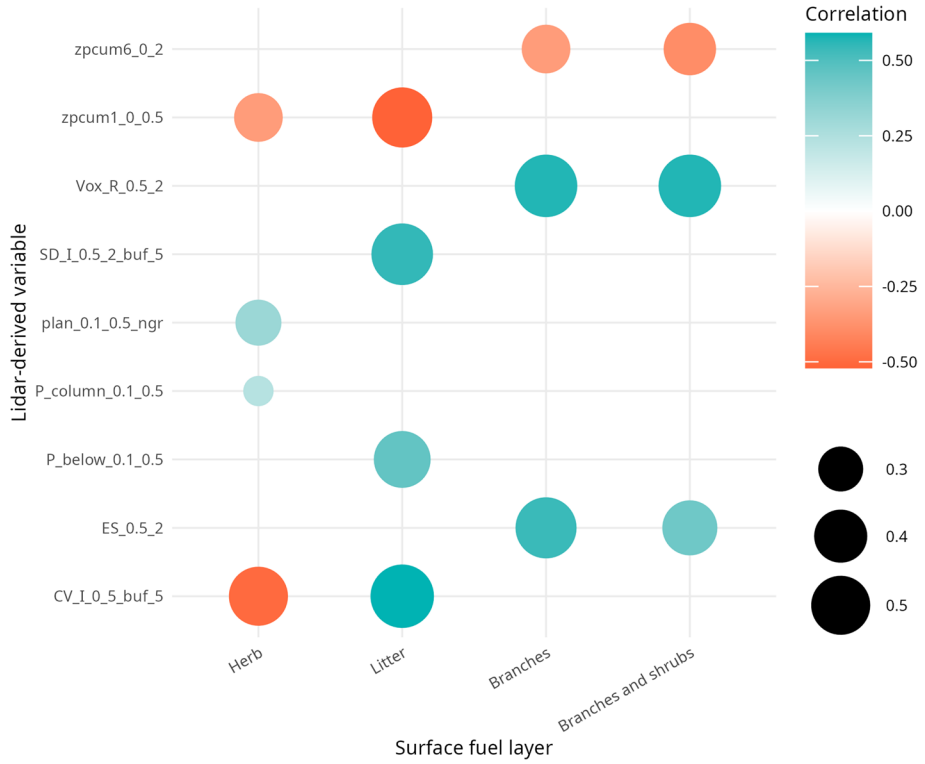

Fig. 4 Pearson correlation coefficients between selected independent lidar-derived metrics and corresponding dependent surface fuel metrics

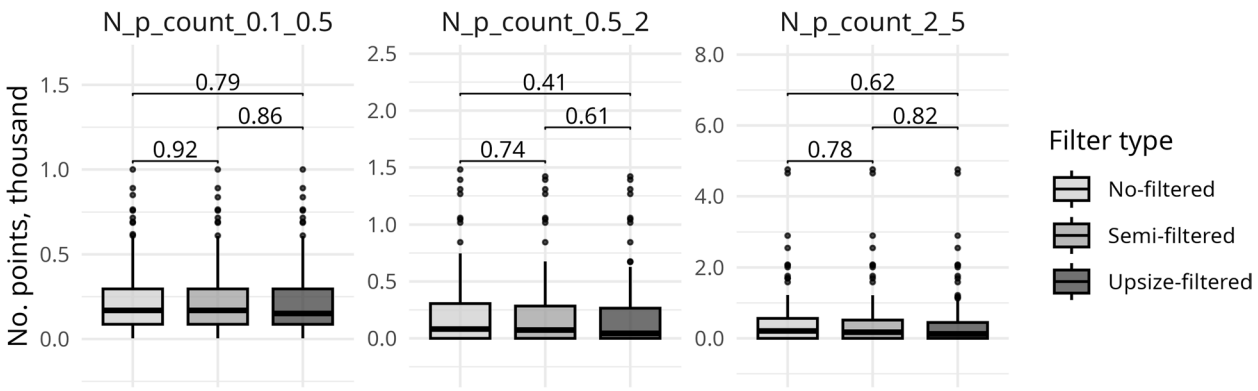

Fig. 5 Impact of trunk filtering on the quantity of lidar returns across height strata

demonstrated the best explanatory ability for litter layer depth ($R^2 = 0.39$). The models explained up to 27% of the variation in the herbaceous layer, up to 28% of the branch biomass in the shrub layer, and up to 28% of the combined biomass of branches and dead shrub stems.

Parametric regressions (LR and NLS) had superior explanatory capabilities compared to the nonparametric RF model (Fig. 7). However, RF demonstrated comparable performance ($\Delta R^2 = \leq 0.02$) for litter layer depth when using non-filtered lidar-derived data. We obtained similar predictive capacity in NLS and LR, which indicates no complex nonlinear relationships between lidar-derived metrics and surface fuel load. Consequently, we present the performance of the LR model as a representative case (Fig. 8), while providing the corresponding scatterplots for the NLS and RF models, as well as a table containing model performance data in the supplementary materials (Fig. S3, Fig. S4. Table S5) for further comparison.

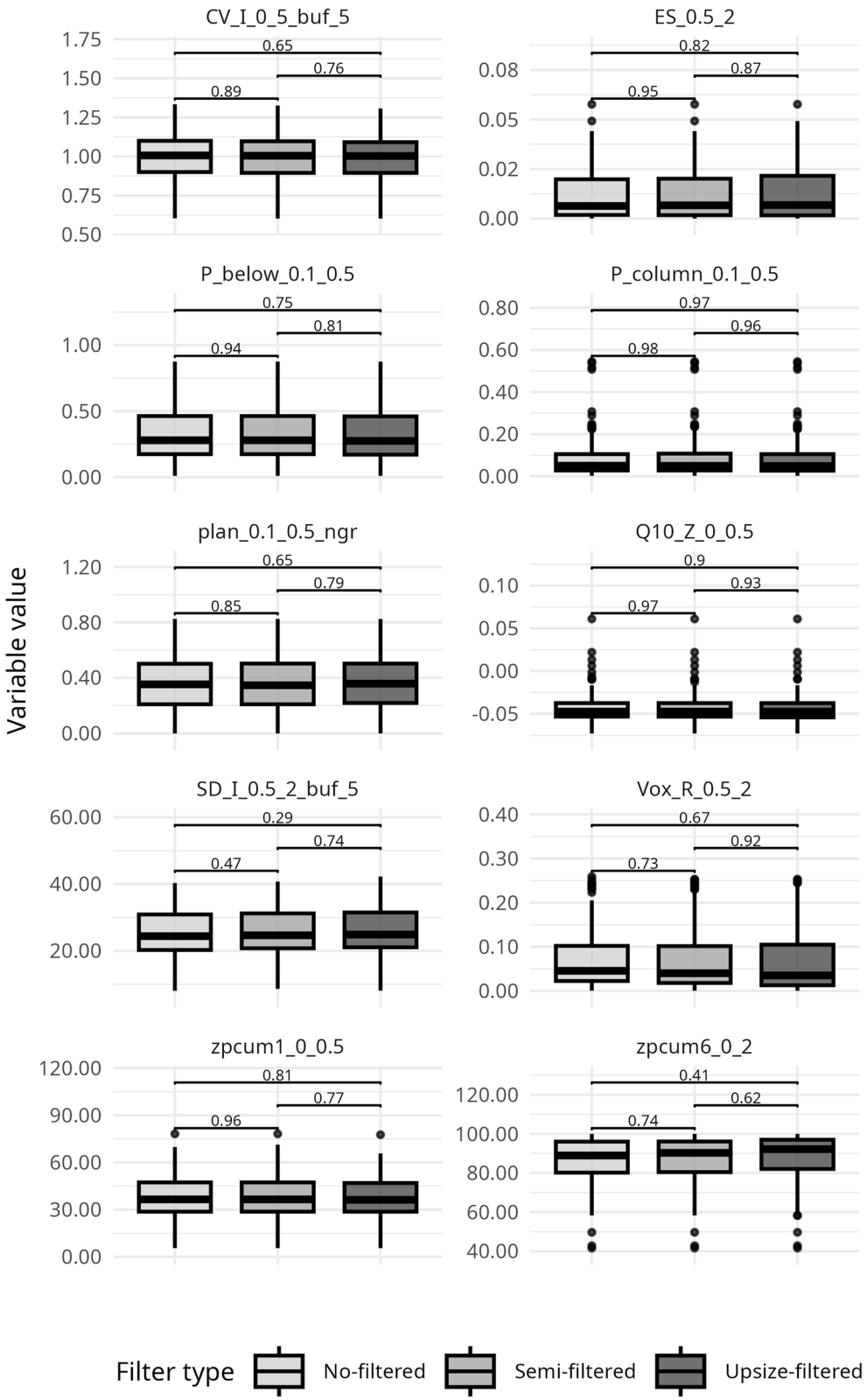

Fig. 6 Impact of filtering tree trunk points on distribution of lidar-derived metrics (Table 2), with *p*-values estimated using Students *t*-test

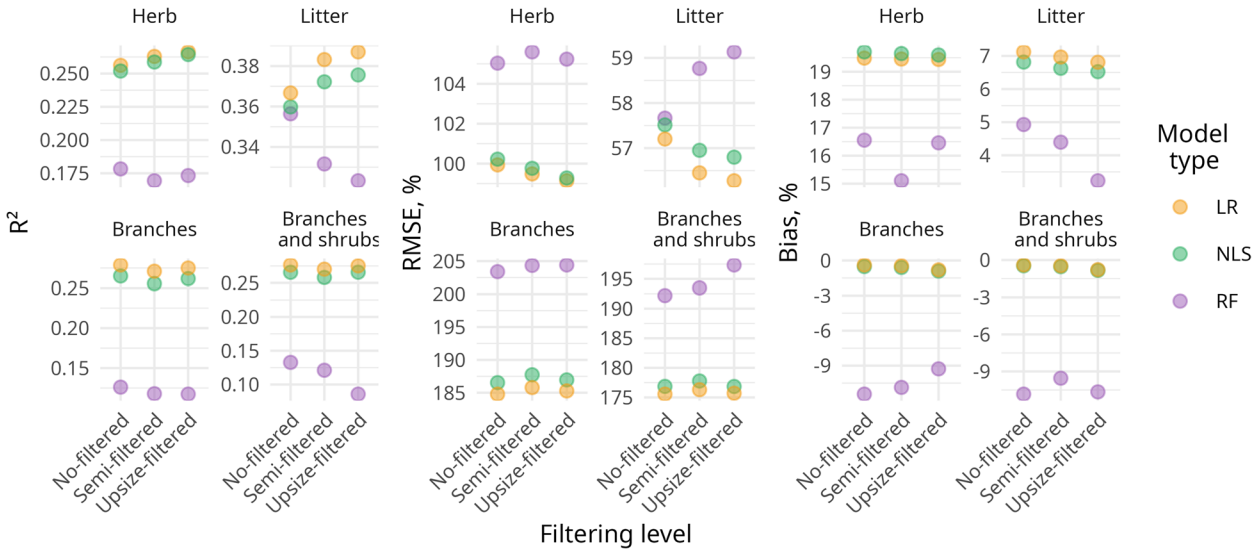

Fig. 7 Model performance indicators across surface fuel components and levels of filtering, as evaluated by leave-one-out cross-validation. RF, random forest; NLS, nonlinear least squares; LR, linear regression

While using parametric models for the litter depth layer, we observed a slight improvement in their explanatory ability as a result of TPF ($\Delta R^2 = 0.02$), while the performance of the RF model decreased (Fig. 7). However, we also observed a decline in *bias* of RF ($\Delta bias = -2\%$) for the litter layer under the utilization of TPF, while the LR and NLS remained at the same level.

TPF did not significantly improve model performance for the corresponding strata (branch biomass and combined shrub–branch biomass), although notable changes in predictor distributions located above 0.5 m height were observed (Fig. 6). The only exception was the RF model, where filtering resulted in reduced explanatory power. In contrast, a nonsignificant improvement was observed for the herbaceous and litter layers using LR ($\Delta R^2 = 0.01$ and 0.02, respectively), likely due to changes in lidar intensity metrics. The intensity metrics showed marginal gains in model performance, since those were calculated within a vertical buffer extending to 5 m above the stratum, where TPF had a more significant effect on the predictors.

Discussion

In this study, we collected ALS data from a low flight altitude, resulting in a high-density point cloud (2354–2913 points m^{-2}). We utilized the unique combination of ALS data and a specifically developed sampling protocol, which involved the establishment of 1-m radius small sample plots. The very high density of the lidar data also enabled us to classify trunk points directly from the point cloud. Our findings highlight that the effect of TPF is not uniform across strata: lidar metrics derived from layers encompassing the surface fuel stratum (up to 2.0 m vertically) and extending up to 5 m above ground level were more sensitive to trunk point filtering, whereas metrics within surface layers remained relatively stable. This pattern may be attributed to occlusion effects, where shrubs, herbaceous vegetation, tree branches, and canopy layer partially obscure tree trunks, limiting their representation in the ALS point cloud and reducing the performance of trunk detection and filtering.

We did not detect any substantial effect of TPF on the performance of surface fuel models. These results suggest that TPF may be unnecessary for large-scale surface fuel modeling using ALS data, saving both processing time and computational resources. Moreover, given that ALS point densities rarely achieve the level of trunk detection attainable with TLS (Donager et al. 2021), avoiding this step provides a more consistent and practical workflow across different forest types without losing accuracy of estimates.

Model performance and limitations

We achieved low to moderate model performances by predicting surface fuels using linear models. We found that the RF model exhibited a higher probability of overestimating small values in comparison to parametric regression methods (Fig. S4), which was not observed when utilizing parametric regression approaches. Additionally, the performance of the RF model for litter fuel component decreased where TPF was applicable. Meanwhile, most studies have utilized the nonparametric

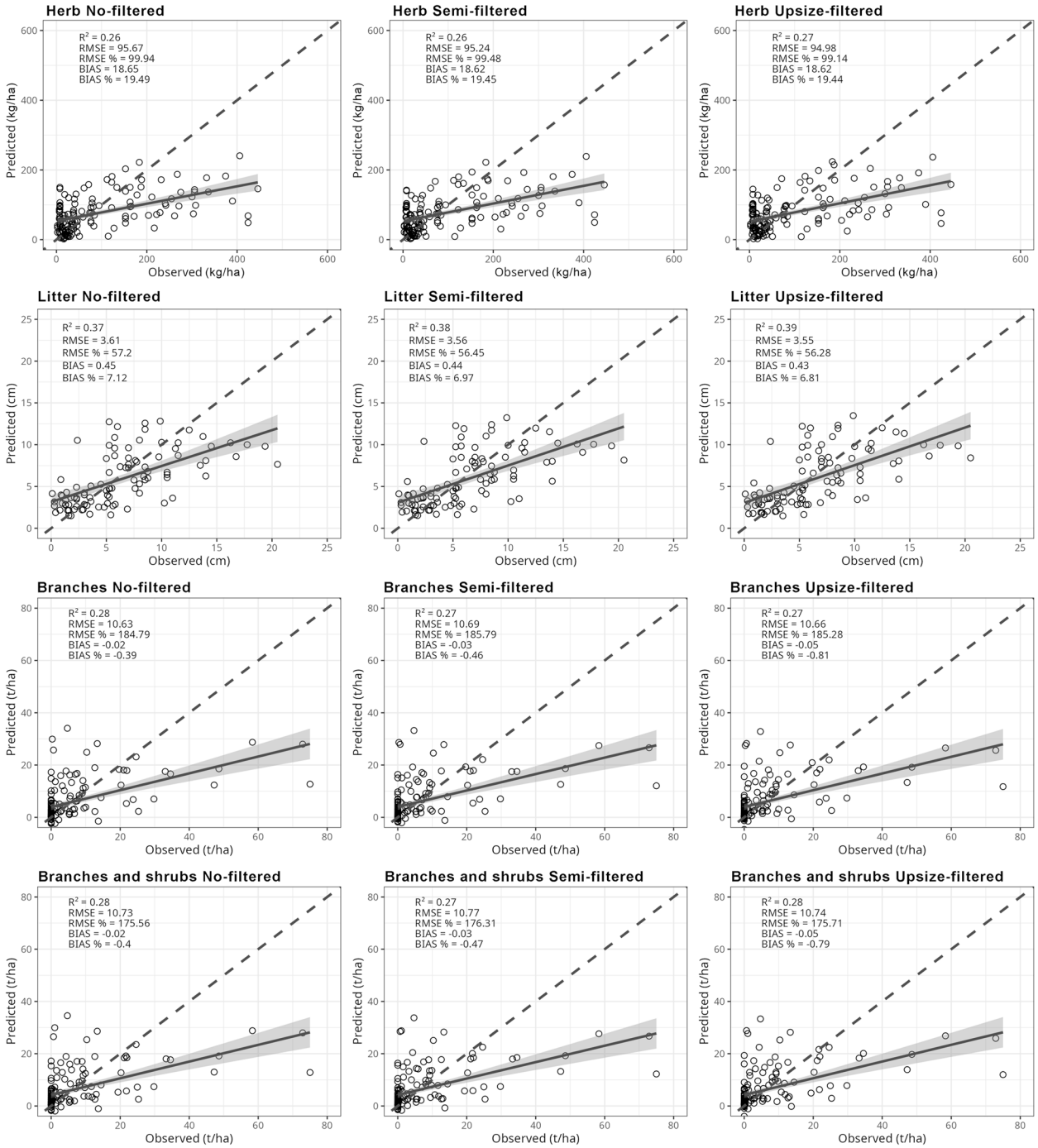

Fig. 8 Performance of linear regression predicting surface fuels across different fuel components and type of trunk points filtering. Dashed line represents a perfect correspondence between observed and modeled data; solid line represents regression between predicted and observed values with 95% confidence interval

regression for modelling surface fuel load, such as RF (Venier et al. 2019; Bright et al. 2022; Labenski et al. 2023; McCarley et al. 2024). Our findings showed that LR outperformed RF regression in predicting surface fuel load, indicating that the relationships between lidar metrics and fuel load are closely linear. This pattern is probably related to several interacting factors: a relatively small sample size, the right-skewed distribution of the surface fuel load data, and the noise of the lidar-derived data (lidar returns contained beams from other fuel

components within strata). These limitations could have reduced the explanatory ability of the RF model; meanwhile, linear regression approaches demonstrated better performance. We therefore caution that this result may not necessarily hold in larger datasets, where machine learning models could potentially demonstrate superior predictive ability.

Litter layer depth in our study was predicted with the best model performance among other fuel components in 0.0–2.0 m vegetation strata ($R^2 = 0.37–0.39$). We revealed a strong correlation between the CV and SD of lidar intensity ($P = 0.55$; 0.59, respectively) calculated within a 5-m radius and litter load. A possible reason for this is that the tree species composition impacts both litter load and spectral reflectivity, as our sites represent diverse boreo-nemoral conditions with mixtures of Scots pine, Norway spruce, European oak, and silver birch. The underlying reason for this phenomenon can be attributed to the dependence of the obtained lidar reflected beam intensity value on the composition of the stand, which in turn directly affects the variability of the fuel load (Martin-Ducup et al. 2025). Other studies have reported diverse results regarding litter model accuracy, finding it more challenging to predict compared to canopy and ladder fuels. For instance, Labenski et al. (2023) estimated litter load with $R^2 = 0.13$ and litter depth with $R^2 = 0.30$. Model accuracies have been shown to vary greatly ($R^2 = 0.19–0.49$) across study areas (Tenny et al. 2025). Meanwhile, Bright et al. (2022) explained 59% of the variation in litter and duff, using a digital elevation model and time since the last fire as additional variables. Lin et al. (2024) described 57% of the variation using point density metrics at stand level, while Stefanidou et al. (2020) described 69% of the variation. McCarley et al. (2024) explained 43% of the litter and 26% of the duff layer variability, which indicates a great potential to deliver accurate site-specific models of litter load.

When working with the group of intensity metrics, we conducted a series of tests on sample plots limited by their radius of 1 m, but we did not find any significant relationship with litter load. The increase of up to 5 m showed a positive correlation in estimating litter depth. The positive correlation between lower vegetation strata and intensity metrics was confirmed by Stefanidou et al. (2020). Simultaneously, the selection of first or all lidar returns did not impact the correlations between independent intensity variables and litter depth.

We predicted the load of herbaceous vegetation with low accuracy ($R^2 = 0.17–0.27$). We expected that our low-altitude flying laser scanner would be able to capture enough points for herbaceous plants in plots with a small size (1 m radius). However, some occlusion by the forest canopy, tree trunks, lower branches of Norway spruce trees, or shrubs likely distorted the signal. TLS can be more helpful in avoiding occlusion. For instance, a study that compared TLS with traditional field surveys to model herbaceous fuels explained 72% of the variation in herbaceous biomass within similar small plots, surpassing lower explanation ability ($R^2 = 0.34$) of conventional measurement methods (Li et al. 2021). TLS data also showed superior performance in other studies (Wallace et al. 2017; Hudak et al. 2020). Modeling performance of herbaceous layer using ALS data demonstrated moderate explanatory ability across studies, with R^2 values ranging from 0.53 (Labenski et al. 2023) to 0.71 (Stefanidou et al. 2020). Both studies utilized an area-based approach for fuel load modeling, where Labenski et al. (2023) also demonstrated dependence mostly on multispectral features and canopy characteristics. Other studies demonstrated low model performance, where only 10.4% variance of herbaceous fuel load was explained (McCarley et al. 2024). Martin-Ducup et al. (2025) also demonstrated the poor relationship ($R^2 = 0.11$) between vegetation coverage in the lower (0.0–0.5 m) stratum and ALS point densities using return density index within the corresponding stratum.

This study relied on direct field measurements of shrub stem diameters, branch diameters and lengths, while previous studies have relied on allometry equations to estimate shrub biomass. We eliminated a common source of uncertainty in branches volume estimation by avoiding the use of allometry equations, ensuring that our models were grounded in observed rather than inferred biomass values. However, an important limitation of our approach is the absence of foliage and needle biomass measurements in the shrub layer, which may have negatively influenced its explanatory power, since lidar pulses are reflected by both woody shrub components and green biomass. In addition, the small size of the sample plots could further limit the model skill. Our study reached 28% of explanatory ability within the 0.5–2.0-m stratum. Shrub biomass strongly depends on local light availability under the forest canopy layer, which can only be reliably assessed with an area-based approach. All other studies utilized a combination of ALS data with data collected using area-based approach, where explanatory ability varied substantially. This variability reflects both the methodological differences and the choice of lidar-derived metrics used to characterize this fuel layer. Labenski et al. (2023) demonstrated a range of explanatory power, with R^2 values of 0.33 for fine shrub fuels and 0.64 for woody shrubs. We also corroborate the findings of Labenski et al. (2023), highlighting the importance of geometric metrics for assessment of this fuel stratum. In our study, cumulative height metrics as well as voxel-based indices (Vox_R_0.5_2) were also significant variables. McCarley

et al. (2024) obtained contrasting results using ALS data (canopy cover, height quartiles, and density metrics alone), where the results yielded limited explanatory ability (explained 7.0% of the variance in the shrub and seedling layer simultaneously) and 31% of the variability of total understory fuels. Martin-Ducup et al. (2025) described 39% and 48% variation of vegetation coverage within 0.5–1.0 and 1.0–2.0-m strata, respectively. In contrast, Tenny et al. (2025) achieved an explanatory power of 53% for total standing surface fuels, which were largely represented by shrubs, using LAD profiles of TLS data.

Our study aimed to investigate the surface fuel load, separated only by components, which is important for wildfire behavior modeling (Scott and Burgan 2005), and we did not assess the model performance for the total value of surface fuel. We assume that the total understory strata predictions are more accurate, as point cloud slices for one fuel component may include laser beams intercepted by another component. For example, any lidar metric at 0.0–0.5-m stratum will include combined signals from litter, herbs, lower parts of long tree branches (e.g., common for Norway spruce), deadwood, and large boulders. The accuracy of predicting understory vegetation by components or altogether varies significantly across studies. Evidently, this way of assessing surface and ladder fuel loads demonstrated enhanced model performance than modeling individual fuel components separately. The model achieved a performance capacity of 49–75% in explaining the variation in total understory biomass using stereophotogrammetric surveying data collected under the forest canopy (Zhang et al. 2022). TLS data reached comparable ($R^2 = 0.61–0.74$) model performance (Loudermilk et al. 2023). As demonstrated by the superior explanatory ability in Post et al. (2025) and Rowell et al. (2020), the models of understory biomass performed well, explaining up to 90%, mostly capitalizing voxel-based metrics.

Variability in micro topography within the sample polygons presented an additional challenge in estimating ground fuels. Stones with a height of up to 0.5 m were common on our sites, and these were not classified as part of the "ground layer" when normalizing the point cloud. We did not assess the impact of stones on the model performance in the present study, although we realize that their presence might affect the values of independent variables (Fig. 9).

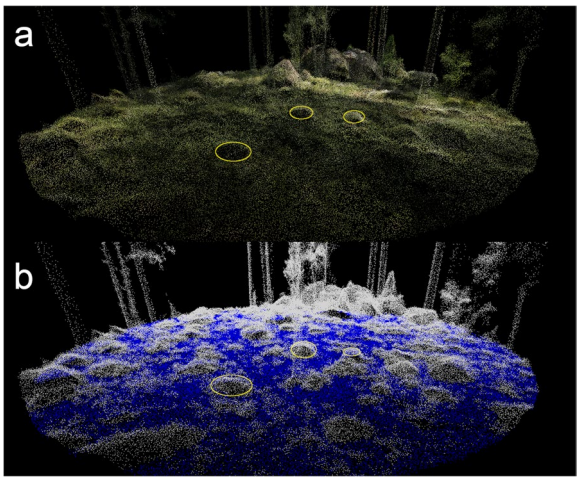

Fig. 9 Illustration of a 10-m ROI surface area of the sample plot, with yellow circles representing stones. **a** RGB-colored point cloud, **b** blue points represent ground-classified returns, while white points represent non-ground returns

Impact of filtering tree trunk points out

Our study was unable to confirm a significant effect of trunk filtering on the performance of surface fuel models. It is important to note that our results were obtained using a unique setup that combines high-density ALS data with small sample plots. Alternative designs, such as area-based approaches with a larger size of sample plots or using TLS data, could obtain different results of TPF impact on model performance. In practice, ALS is primarily suited to area-based assessments rather than trunk classification (White et al. 2016), and our findings provide evidence that pursuing extremely high-density ALS solely for stem delineation is not essential, as this does not substantially affect the predictive performance of surface fuel models. To date, the utilization of TPF approach in studies has been limited, with only few studies employing this method. For instance, Tenny et al. (2025) conducted a removal of non-foliage vegetation during LAD assessment. Adhikari et al. (2023) utilized a tree stem filtering approach on TLS data, which explained comparatively 80% of the total surface fuel variation. In the study by Zhang et al. (2022), stereophotogrammetrical data under the canopy layer was applied, with points located at > 2-m height (representing non-understory vegetation) being filtered out. Jarron et al. (2020) applied a similar approach to limit their lidar point cloud only to understory layer. The potential utility and implications of these classifications remain unclear. The ability to characterize understory strata using ALS data was also declining under occlusion impact (Venier et al. 2019), but no confirmed impact on model performance results has been demonstrated.

Conclusions

The utilization of ALS data holds considerable promise in the estimation of fuel loads under the canopy of boreal forests. Our study highlights the computation complexities in modeling forest surface fuels. Despite the use of

very high-density ALS data from low flight altitudes in combination with small sample plots, the capacity to describe surface fuel load remained inferior to that could be achieved by TLS data, which better captures structural complexity of the forest understory. Our findings indicate that litter-related metrics primarily depend on stand-level data, which explains the need for increased plot radius to achieve better performance of estimates. Simultaneously, small-radius sample plots are essential for capturing fine-scale fuel variability in forest stands, such as shrub and herbaceous biomass. Thus, achieving ALS performance comparable to TLS requires a point cloud with density exceeding 3000 points m^{-2}. At such densities, ALS-based models still have lower explanatory power than TLS applications (> 10,000 points m^{-2}). However, UAV-based laser scanning retains a key advantage by providing spatially explicit estimates of surface fuel load across large areas. This enables the characterization of within-stand heterogeneity of surface fuels and supports spatially continuous fuel mapping, which is difficult to achieve with TLS due to its limited spatial coverage and operational constraints. Further works should estimate wider impact of the TPF methodologies employed, with diverse lidar data and forest types, in addition to varied sample plot establishment techniques.

Abbreviations

3D	Three-dimensional
ALS	Airborne laser scanning
CBH	Canopy base height
LiDAR	Lidar Light Identification, Detection and Ranging
LR	Linear least squares regression
LOOCV	Leave-one-out cross-validation
NLS	Nonlinear least squares regression
RF	Random forest
RGB	Red, green, and blue
RTK	Real-time kinematics
ROI	Region of interest
TLS	Terrestrial laser scanning
TPF	Trunk points filtering
UAV	Unmanned aerial vehicle

Supplementary Information

The online version contains supplementary material available at https://doi.org/10.1186/s42408-026-00454-y.

Additional file 1: Fig. S1. Empirical cumulative distribution functions (ECDF) of lidar-derived variable distributions under different filter type. Fig. S2. Impact of tree TPF on distribution of lidar-derived metrics, with p-values estimated using paired Students t-test. Fig. S3. Performance of NLS (Nonlinear Least Squares) predicting surface fuels across different fuel components and type of trunks points filter. Dashed line represent a perfect correspondence between observed and modeled data; solid line represents regression between predicted and observed values with 95% confidence interval. Fig. S4. Performance of RF (Random Forest) predicting surface fuels across different fuel components and type of trunks points filter. Dashed line represent a perfect correspondence between observed and modeled data; solid line represents regression between predicted and observed values with 95% confidence interval. Table S5. Model performance parameters across surface fuel components and levels of filtering, as evaluated by Leave-one-out cross-validation.

Authors' contributions
Conceptualization: MM; methodology: RZ and MM; formal analysis and investigation: RZ and OW; writing and preparation of the original draft: RZ, MM and OW; writing, review, and editing: RZ, MM, IG; funding acquisition: MM and IG. All authors have read and approved the final manuscript.

Funding
This study was carried out within the project "Development of LIDAR-based protocol for forest fuel assessment and fire effects to support conservation burns in southern Swedish oak forests (L-BURNS)" funded by Crafoord Foundation (No. 20241054). ID was additionally supported by Foundation for the Memory of Oskar Lilli Lamms (project no. DO2024-0012), FORMAS (no. 2023–02509), and Foundation Partnerskap Alnarp.

Data availability
Data collected within this study, the code developed for this study, as well as developed allometry equations will be available upon request from the authors.

Declarations

Ethics approval and consent to participate
The authors declare that they have no known competing financial interests or personal relationships that could have influenced the work reported in this paper. All authors have read, understood, and, as applicable, complied with the statement on the "Ethical Responsibilities of Authors" as outlined in the Instructions for Authors. They are aware that with minor exceptions, no changes can be made to the authorship once the paper is submitted.

Consent for publication
All authors give their consent to publication.

Competing interests
The authors declare no competing interests.

Author details
[1]National University of Life and Environmental Sciences of Ukraine, Heroiv Oborony Street, 15, Kyiv 03041, Ukraine. [2]Southern Swedish Forest Research Centre, Swedish University of Agricultural Sciences, Sundsvägen 3, Alnarp 23456, Sweden.

Received: 29 September 2025 Accepted: 4 February 2026
Published online: 21 February 2026

References

Almeida, Danilo Roberti Alves De, Scott Christopher Stark, Carlos Alberto Silva, Caio Hamamura, and Ruben Valbuena. 2019. 'leafR: calculates the leaf area index (LAD) and other related functions'. June 11. https://doi.org/10.32614/CRAN.package.leafR.

Adhikari, Angel, Alicia Peduzzi, Cristian R.. Montes, Nathaniel Osborne, and Deepak R.. Mishra. 2023. Assessment of understory vegetation in a plantation forest of the Southeastern United States using terrestrial laser scanning. *Ecological Informatics* 77 : 102254. https://doi.org/10.1016/j.ecoinf.2023.102254.

Åkerblom, Markku, and Pekka Kaitaniemi. 2021. Terrestrial laser scanning: A new standard of forest measuring and modelling? *Annals of Botany* 128 (6): 653–662. https://doi.org/10.1093/aob/mcab111.

An, Zhongming, and Roberte Froese. 2023. Tree stem volume estimation from terrestrial LiDAR point cloud by unwrapping. *Canadian Journal of Forest Research* 53 (2): 60–70. https://doi.org/10.1139/cjfr-2022-0153.

Andersen, Hans-Erik., Robert J.. McGaughey, and Stephen E.. Reutebuch. 2005. Estimating forest canopy fuel parameters using LiDAR data. *Remote Sensing of Environment* 94 (4): 441–449. https://doi.org/10.1016/j.rse.2004.10.013.

Arkin, Jeremy, Nicholas C. Coops, Lori D. Daniels, and Andrew Plowright. 2025. Canopy and surface fuel estimations using RPAS and ground-based point clouds. *Forestry: An International Journal of Forest Research* 98 (1): 15–28. https://doi.org/10.1093/forestry/cpad020.

Arrizza, S., S. Marras, R. Ferrara, and G. Pellizzaro. 2024. Terrestrial laser scanning (TLS) for tree structure studies: A review of methods for wood-leaf classifications from 3D point clouds. *Remote Sensing Applications: Society and Environment* 36 : 101364. https://doi.org/10.1016/j.rsase.2024.101364.

Balenović, Ivan, Xinlian Liang, Luka Jurjević, Juha Hyyppä, Ante Seletković, and Antero Kukko. 2021. Hand-held personal laser scanning: Current status and perspectives for forest inventory application. *Croatian Journal of Forest Engineering* 42 (1): 165–183. https://doi.org/10.5552/crojfe.2021.858.

Barros, Ana M. G.., Alan A.. Ager, Michelle A.. Day, Meg A.. Krawchuk, and Thomas A.. Spies. 2018. Wildfires managed for restoration enhance ecological resilience. *Ecosphere*. https://doi.org/10.1002/ecs2.2161.

Bauwens, Sébastien., Harm Bartholomeus, Kim Calders, and Philippe Lejeune. 2016. Forest inventory with terrestrial LiDAR: A comparison of static and hand-held mobile laser scanning. *Forests* 7 (6) : 127. https://doi.org/10.3390/f7060127.

Bouvier, Marc, Sylvie Durrieu, Frédéric. Gosselin, and Basile Herpigny. 2017. Use of airborne LiDAR data to improve plant species richness and diversity monitoring in lowland and mountain forests. *PLoS ONE* 12 (9) : e0184524. https://doi.org/10.1371/journal.pone.0184524.

Bright, Benjamin C.., Andrew T.. Hudak, T. Ryan. McCarley, et al. 2022. Multitemporal LiDAR captures heterogeneity in fuel loads and consumption on the Kaibab Plateau. *Fire Ecology*. https://doi.org/10.1186/s42408-022-00142-7.

Brown, James K. 1974. *Handbook for Inventorying Downed Woody Material*. INT-16. US Department of Agriculture, Forest Service, Intermountain Forest and Range Experiment Station.

Calders, Kim, Jennifer Adams, John Armston, et al. 2020. Terrestrial laser scanning in forest ecology: Expanding the horizon. *Remote Sensing of Environment* 251 : 112102. https://doi.org/10.1016/j.rse.2020.112102.

Cameron, H. A., D. Schroeder, and J. L. Beverly. 2022. Predicting black spruce fuel characteristics with airborne laser scanning (ALS). *International Journal of Wildland Fire* 31 (2): 124–135. https://doi.org/10.1071/WF21004.

Cardil, Adrián, Santiago Monedero, Gavin Schag, et al. 2021. Fire behavior modeling for operational decision-making. *Current Opinion in Environmental Science & Health* 23 : 100291. https://doi.org/10.1016/j.coesh.2021.100291.

Catchpole, W. R., and C. J. Wheeler. 1992. Estimating plant biomass: A review of techniques. *Australian Journal of Ecology* 17 (2): 121–131. https://doi.org/10.1111/j.1442-9993.1992.tb00790.x.

Chen, Shilin, Hans Verbeeck, Louise Terryn, et al. 2025. The impact of leaf-wood separation algorithms on aboveground biomass estimation from terrestrial laser scanning. *Remote Sensing of Environment* 318 (March) : 114581. https://doi.org/10.1016/j.rse.2024.114581.

Cimdins, Reinis, Tuomas Yrttimaa, Juha Hyyppä, Mikko Vastaranta, and Ville Kankare. 2025. Capturing trends in forest structural complexity development using laser scanning techniques. *Trees, Forests and People* 21 (September) : 100954. https://doi.org/10.1016/j.tfp.2025.100954.

De Conto, Tiago, Kenneth Olofsson, Eric Bastos Görgens, Luiz Carlos Estraviz. Rodriguez, and Gustavo Almeida. 2017. Performance of stem denoising and stem modelling algorithms on single tree point clouds from terrestrial laser scanning. *Computers and Electronics in Agriculture* 143 (December): 165–176. https://doi.org/10.1016/j.compag.2017.10.019.

Donager, Jonathon J.., Andrew J.. Sánchez Meador, and Ryan C.. Blackburn. 2021. Adjudicating perspectives on forest structure: How do airborne, terrestrial, and mobile LiDAR-derived estimates compare? *Remote Sensing* 13 (12) : 2297. https://doi.org/10.3390/rs13122297.

Du, Liming, and Yong Pang. 2024. Identifying regenerated saplings by stratifying forest overstory using airborne LiDAR data. *Plant Phenomics* 6 : 0145. https://doi.org/10.34133/plantphenomics.0145.

Ellis, Todd M.., David M. J. S.. Bowman, Piyush Jain, Mike D.. Flannigan, and Grant J.. Williamson. 2022. Global increase in wildfire risk due to climate-driven declines in fuel moisture. *Global Change Biology* 28 (4): 1544–1559. https://doi.org/10.1111/gcb.16006.

Flynn, William Rupert Moore., Harry Jon Foord. Owen, Stuart William David. Grieve, and Emily Rebecca Lines. 2023. Quantifying vegetation indices using terrestrial laser scanning: Methodological complexities and ecological insights from a Mediterranean forest. *Biogeosciences* 20 (13): 2769–2784. https://doi.org/10.5194/bg-20-2769-2023.

Forbes, Brieanne, Sean Reilly, Matthew Clark, et al. 2022. Comparing remote sensing and field-based approaches to estimate ladder fuels and predict wildfire burn severity. *Frontiers in Forests and Global Change*. https://doi.org/10.3389/ffgc.2022.818713.

Gale, Matthew G.., Geoffrey J.. Cary, Albert I.J.M.. Van Dijk, and Marta Yebra. 2021. Forest fire fuel through the lens of remote sensing: Review of approaches, challenges and future directions in the remote sensing of biotic determinants of fire behaviour. *Remote Sensing of Environment* 255 : 112282. https://doi.org/10.1016/j.rse.2020.112282.

Hall, Sonia A.., and Ingrid C.. Burke. 2006. Considerations for characterizing fuels as inputs for fire behavior models. *Forest Ecology and Management* 227 (1–2): 102–114. https://doi.org/10.1016/j.foreco.2006.02.022.

Hamraz, Hamid, Marco A. Contreras, and Jun Zhang. 2017. *Vertical stratification of forest canopy for segmentation of under-story trees within small-footprint airborne LiDAR point clouds*. Version 4. https://doi.org/10.48550/ARXIV.1701.00169.

Hawley, Christie M.., E. Louise. Loudermilk, Eric M.. Rowell, and Scott Pokswinski. 2018. A novel approach to fuel biomass sampling for 3D fuel characterization. *MethodsX* 5:1597–1604. https://doi.org/10.1016/j.mex.2018.11.006.

Heinaro, Einari, Topi Tanhuanpää, Tuomas Yrttimaa, Markus Holopainen, and Mikko Vastaranta. 2021. Airborne laser scanning reveals large tree trunks on forest floor. *Forest Ecology and Management* 491 (July) : 119225. https://doi.org/10.1016/j.foreco.2021.119225.

Hudak, Andrew T., Akira Kato, Benjamin C. Bright, et al. 2020. Towards spatially explicit quantification of pre- and postfire fuels and fuel consumption from traditional and point cloud measurements. *Forest Science* 66 (4): 428–442. https://doi.org/10.1093/forsci/fxz085.

Hyyppä, Eric, Xiaowei Yu, Harri Kaartinen, et al. 2020. Comparison of backpack, handheld, under-canopy UAV, and above-canopy UAV laser scanning for field reference data collection in boreal forests. *Remote Sensing* 12 (20) : 3327. https://doi.org/10.3390/rs12203327.

Iglesias, Virginia, Jennifer K.. Balch, and William R.. Travis. 2022. U.S. fires became larger, more frequent, and more widespread in the 2000s. *Science Advances*. https://doi.org/10.1126/sciadv.abc0020.

Jakubowksi, Marek K.., Qinghua Guo, Brandon Collins, Scott Stephens, and Maggi Kelly. 2013. Predicting surface fuel models and fuel metrics using LiDAR and CIR imagery in a dense, mountainous forest. *Photogrammetric Engineering & Remote Sensing* 79 (1): 37–49. https://doi.org/10.14358/pers.79.1.37.

Jalkanen, Anneli, Raisa Mäkipää, Göran. Ståhl, Aleksi Lehtonen, and Hans Petersson. 2005. Estimation of the biomass stock of trees in Sweden: Comparison of biomass equations and age-dependent biomass expansion factors. *Annals of Forest Science* 62 (8): 845–851. https://doi.org/10.1051/forest:2005075.

Jarron, Lukas R.., Nicholas C.. Coops, William H.. MacKenzie, Piotr Tompalski, and Pamela Dykstra. 2020. Detection of sub-canopy forest structure using airborne LiDAR. *Remote Sensing of Environment* 244 : 111770. https://doi.org/10.1016/j.rse.2020.111770.

Jones, Matthew W.., John T.. Abatzoglou, Sander Veraverbeke, et al. 2022. Global and regional trends and drivers of fire under climate change. *Reviews of Geophysics*. https://doi.org/10.1029/2020rg000726.

Keane, Robert E. 2013. Describing wildland surface fuel loading for fire management: A review of approaches, methods and systems. *International Journal of Wildland Fire* 22 (1): 51–62. https://doi.org/10.1071/WF11139.

Keane, Robert E. 2015. Wildland fuel fundamentals and applications. *Springer International Publishing*. https://doi.org/10.1007/978-3-319-09015-3.

Labenski, Pia, Michael Ewald, Sebastian Schmidtlein, Faith Ann Heinsch, and Fabian Ewald Fassnacht. 2023. Quantifying surface fuels for fire modelling in temperate forests using airborne LiDAR and Sentinel-2: Potential and limitations. *Remote Sensing of Environment* 295 : 113711. https://doi.org/10.1016/j.rse.2023.113711.

Laino, Diego, Carlos Cabo, Covadonga Prendes, et al. 2024. 3DFin: A software for automated 3D forest inventories from terrestrial point clouds. *Forestry: An International Journal of Forest Research* 97 (4): 479–496. https://doi.org/10.1093/forestry/cpae020.

Lesmeister, Damon B.., Stan G.. Sovern, Raymond J.. Davis, David M.. Bell, Matthew J.. Gregory, and Jody C.. Vogeler. 2019. Mixed-severity wildfire and habitat of an old-forest obligate. *Ecosphere*. https://doi.org/10.1002/ecs2.2696.

Li, Shun, Tianming Wang, Zhengyang Hou, Yinan Gong, Limin Feng, and Jianping Ge. 2021. Harnessing terrestrial laser scanning to predict understory

biomass in temperate mixed forests. *Ecological Indicators* 121 : 107011. https://doi.org/10.1016/j.ecolind.2020.107011.

Lin, Di., Vincenzo Giannico, Raffaele Lafortezza, Giovanni Sanesi, and Mario Elia. 2024. Use of airborne LiDAR to predict fine dead fuel load in Mediterranean forest stands of Southern Europe. *Fire Ecology*. https://doi.org/10.1186/s42408-024-00287-7.

Loudermilk, E. Louise., Joseph J.. O'Brien, Robert J.. Mitchell, et al. 2012. Linking complex forest fuel structure and fire behaviour at fine scales. *International Journal of Wildland Fire* 21 (7) : 882. https://doi.org/10.1071/wf10116.

Loudermilk, Eva Louise, Scott Pokswinski, Christie M.. Hawley, et al. 2023. Terrestrial laser scan metrics predict surface vegetation biomass and consumption in a frequently burned southeastern U.S. ecosystem. *Fire* 6 (4) : 151. https://doi.org/10.3390/fire6040151.

Lutes, Duncan C., Robert E. Keane, John F. Caratti, et al. 2006. *FIREMON: Fire Effects Monitoring and Inventory System*. U.S. Department of Agriculture, Forest Service, Rocky Mountain Research Station. https://doi.org/10.2737/rmrs-gtr-164.

Maltamo, Matti, J. Räty, L. Korhonen, et al. 2020. Prediction of forest canopy fuel parameters in managed boreal forests using multispectral and unispectral airborne laser scanning data and aerial images. *European Journal of Remote Sensing* 53 (1): 245–257. https://doi.org/10.1080/22797254.2020.1816142.

Maltamo, M., P. Packalen, L. Laukkanen, and L. Korhonen. 2025. The transferability and cross-use of airborne laser scanning-based leaf-off and leaf-on biomass models. *European Journal of Remote Sensing* 58 (1) : 2542870. https://doi.org/10.1080/22797254.2025.2542870.

Martin-Ducup, Olivier, Jean-Luc. Dupuy, Maxime Soma, et al. 2025. Unlocking the potential of airborne LiDAR for direct assessment of fuel bulk density and load distributions for wildfire hazard mapping. *Agricultural and Forest Meteorology* 362 (March) : 110341. https://doi.org/10.1016/j.agrformet.2024.110341.

McCarley, T. Ryan., Crystal A. Kolden, Nicole M. Vaillant, et al. 2017. Multi-temporal LiDAR and Landsat quantification of fire-induced changes to forest structure. *Remote Sensing of Environment* 191 (March): 419–432. https://doi.org/10.1016/j.rse.2016.12.022.

McCarley, T. Ryan., Andrew T.. Hudak, Benjamin C.. Bright, et al. 2024. Generating fuel consumption maps on prescribed fire experiments from airborne laser scanning. *International Journal of Wildland Fire*. https://doi.org/10.1071/WF23160.

Myroniuk, Viktor, Sergiy Zibtsev, Vadym Bogomolov, et al. 2023. Combining Landsat time series and GEDI data for improved characterization of fuel types and canopy metrics in wildfire simulation. *Journal of Environmental Management* 345 (November) : 118736. https://doi.org/10.1016/j.jenvman.2023.118736.

North, Malcolm P.., Ryan E.. Tompkins, Alexis A.. Bernal, Brandon M.. Collins, Scott L.. Stephens, and Robert A.. York. 2022. Operational resilience in Western US frequent-fire forests. *Forest Ecology and Management* 507 (March) : 120004. https://doi.org/10.1016/j.foreco.2021.120004.

Pelt, Robert Van, and Jerry F. Franklin. 2000. Influence of canopy structure on the understory environment in tall, old-growth, conifer forests. *Canadian Journal of Forest Research* 30 (8): 1231–1245. https://doi.org/10.1139/x00-050.

Penner, Margaret, Joanne C. White, and Murray E. Woods. 2024. Automated characterization of forest canopy vertical layering for predicting forest inventory attributes by layer using airborne LiDAR data. *Forestry: An International Journal of Forest Research* 97 (1): 59–75. https://doi.org/10.1093/forestry/cpad033.

Post, Alanna J., Brieanne Forbes, Zane Cooper, et al. 2025. Using handheld mobile laser scanning to quantify fine-scale surface fuels and detect changes post-disturbance in Northern California forests. *Ecological Indicators* 172 (March) : 113276. https://doi.org/10.1016/j.ecolind.2025.113276.

Prichard, Susan J.., Nicholas A.. Povak, Maureen C.. Kennedy, and David W.. Peterson. 2020. Fuel treatment effectiveness in the context of landform, vegetation, and large, wind-driven wildfires. *Ecological Applications* 30 (5) : e02104. https://doi.org/10.1002/eap.2104.

R Core Team. 2025. *R: a language and environment for statistical computing*. V. 4.5.0. R Foundation for Statistical Computing, released. https://www.r-project.org/.

Ross, C. Wade, E. Louise Loudermilk, Joseph J. O'Brien, et al. 2024. 'LiDAR-derived estimates of forest structure in response to fire frequency'. *Fire Ecology* 20 (1): 44. https://doi.org/10.1186/s42408-024-00279-7.

Roussel, Jean-Romain., David Auty, Nicholas C. Coops, et al. 2020. lidR: An R package for analysis of airborne laser scanning (ALS) data. *Remote Sensing of Environment* 251 (December) : 112061. https://doi.org/10.1016/j.rse.2020.112061.

Rowell, Eric, E. Louise Loudermilk, Christie Hawley, et al. 2020. Coupling terrestrial laser scanning with 3D fuel biomass sampling for advancing wildland fuels characterization. *Forest Ecology and Management* 462 (April) : 117945. https://doi.org/10.1016/j.foreco.2020.117945.

Ryding, Joseph, Emily Williams, Martin Smith, and Markus Eichhorn. 2015. Assessing handheld mobile laser scanners for forest surveys. *Remote Sensing* 7 (1): 1095–1111. https://doi.org/10.3390/rs70101095.

Sánchez-López, Nuria, Andrew T. Hudak, Luigi Boschetti, et al. 2023. A spatially explicit model of tree leaf litter accumulation in fire maintained longleaf pine forests of the Southeastern US. *Ecological Modelling* 481 (July) : 110369. https://doi.org/10.1016/j.ecolmodel.2023.110369.

Sánchez-López, N., A. T. Hudak, M. K. Taylor, M. A. Callaham, and Joseph J.. O'Brien. 2025. Is this duff? Long-term prescribed burning effects on litter and duff in pine flatwoods of the Southeastern US. *Fire Ecology*. https://doi.org/10.1186/s42408-025-00425-9.

Scott, Joe H., and Robert E. Burgan. 2005. *Standard fire behavior fuel models: a comprehensive set for use with Rothermel's surface fire spread model*. RMRS-GTR-153. U.S. Department of Agriculture, Forest Service, Rocky Mountain Research Station. https://doi.org/10.2737/RMRS-GTR-153.

Seidl, Rupert, and Monica G.. Turner. 2022. Post-disturbance reorganization of forest ecosystems in a changing world. *Proceedings of the National Academy of Sciences*. https://doi.org/10.1073/pnas.2202190119.

Seidl, Rupert, Mária. Potterf, Jörg. Müller, Monica G.. Turner, and Werner Rammer. 2024. Patterns of early post-disturbance reorganization in Central European forests. *Proceedings of the Royal Society B: Biological Sciences*. https://doi.org/10.1098/rspb.2024.0625.

Shapiro, S. S., and M. B. Wilk. 1965. An analysis of variance test for normality (complete samples). *Biometrika* 52 (3–4): 591–611. https://doi.org/10.1093/biomet/52.3-4.591.

Sjörs, H. 1963. 'Amphi-Atlantic zonation, nemoral to Arctic'. In *North Atlantic Biota and Their History*, edited by A. Löve and D. Löve. Oxford University Press.

Skowronski, Nicholas S.., Kenneth L.. Clark, Matthew Duveneck, and John Hom. 2011. Three-dimensional canopy fuel loading predicted using upward and downward sensing LiDAR systems. *Remote Sensing of Environment* 115 (2) : 2. https://doi.org/10.1016/j.rse.2010.10.012.

SMHI. 2025. 'Ladda Ner Väderobservationer'. https://www.smhi.se/data/hitta-data-for-en-plats/ladda-ner-vaderobservationer.

Stefanidou, Alexandra, Ioannis Z.. Gitas, Lauri Korhonen, Nikos Georgopoulos, and Dimitris Stavrakoudis. 2020. Multispectral LiDAR-based estimation of surface fuel load in a dense coniferous forest. *Remote Sensing* 12 (20) : 3333. https://doi.org/10.3390/rs12203333.

Stephens, Scott L., Neil Burrows, Alexander Buyantuyev, et al. 2014. Temperate and boreal forest mega-fires: Characteristics and challenges. *Frontiers in Ecology and the Environment* 12 (2): 115–122. https://doi.org/10.1890/120332.

Stone, M. 1974. Cross-validatory choice and assessment of statistical predictions. *Journal of the Royal Statistical Society, B (Methodological)* 32 (2): 111–147.

Student. 1908. 'The probable error of a mean'. *Biometrika* 6 (1): 1. https://doi.org/10.2307/2331554.

Tenny, Johnathan T.., Temuulen Tsagaan Sankey, Seth M.. Munson, Andrew J.. Sánchez Meador, and Scott J.. Goetz. 2025. Canopy and surface fuels measurement using terrestrial LiDAR single-scan approach in the Mogollon Highlands of Arizona. *International Journal of Wildland Fire*. https://doi.org/10.1071/wf24221.

Valbuena, Rubén, Petteri Packalén, Susana Martı´n-Fernández, and Matti Maltamo. 2012. Diversity and equitability ordering profiles applied to study forest structure. *Forest Ecology and Management* 276:185–195. https://doi.org/10.1016/j.foreco.2012.03.036.

Venier, Lisa A., Tom Swystun, Marc J. Mazerolle, et al. 2019. Modelling vegetation understory cover using LiDAR metrics. *PLoS ONE* 14 (11) : e0220096. https://doi.org/10.1371/journal.pone.0220096.

Viedma, O., C. A. Silva, J. M. Moreno, and A. T. Hudak. 2024. LadderFuelsR: A new automated tool for vertical fuel continuity analysis and crown base height detection using light detection and ranging. *Methods in Ecology and Evolution* 15 (11): 1958–1967. https://doi.org/10.1111/2041-210X.14427.

Wallace, Luke, Vaibhav Gupta, Karin Reinke, and Simon Jones. 2016. An assessment of pre- and post fire near surface fuel hazard in an Australian dry sclerophyll forest using point cloud data captured using a terrestrial laser scanner. *Remote Sensing* 8 (8) : 679. https://doi.org/10.3390/rs8080679.

Wallace, Luke, Samuel Hillman, Karin Reinke, and Bryan Hally. 2017. Non-destructive estimation of above-ground surface and near-surface biomass using 3D terrestrial remote sensing techniques. *Methods in Ecology and Evolution* 8 (11): 1607–1616. https://doi.org/10.1111/2041-210X.12759.

Wepryk, Olga, Mats Niklasson, Erik Nordlind, and Igor Drobyshev. 2025. Modelling of forest fuel and weather effects on fire behavior in the oak forests of southern Sweden. *Scandinavian Journal of Forest Research*. https://doi.org/10.1080/02827581.2025.2531994.

White, Joanne C., John T. T. R. Arnett, Michael A. Wulder, Piotr Tompalski, and Nicholas C. Coops. 2015. 'Evaluating theImpact of Leaf-on and Leaf-off Airborne Laser Scanning Data on the Estimation of Forest Inventory Attributes with the Area-Based Approach'. *Canadian Journal of Forest Research* 45(11):1498–513. https://doi.org/10.1139/cjfr-2015-0192.

White, Joanne C.., Nicholas C.. Coops, Michael A.. Wulder, Mikko Vastaranta, Thomas Hilker, and Piotr Tompalski. 2016. Remote sensing technologies for enhancing forest inventories: A review. *Canadian Journal of Remote Sensing* 42 (5): 5. https://doi.org/10.1080/07038992.2016.1207484.

Woodgate, William, John D. Armston, Mathias Disney, et al. 2016. Quantifying the impact of woody material on leaf area index estimation from hemispherical photography using 3D canopy simulations. *Agricultural and Forest Meteorology* 226–227 (October): 1–12. https://doi.org/10.1016/j.agrformet.2016.05.009.

Wulder, Michael A., David P. Roy, Volker C. Radeloff, et al. 2022. Fifty years of Landsat science and impacts. *Remote Sensing of Environment* 280 (October) : 113195. https://doi.org/10.1016/j.rse.2022.113195.

Xi, Zhouxin, Laura Chasmer, and Chris Hopkinson. 2023. Delineating and reconstructing 3D forest fuel components and volumes with terrestrial laser scanning. *Remote Sensing* 15 (19) : 4778. https://doi.org/10.3390/rs15194778.

Zhang, Yupan, Yuichi Onda, Hiroaki Kato, Bin Feng, and Takashi Gomi. 2022. Understory biomass measurement in a dense plantation forest based on drone-SfM data by a manual low-flying drone under the canopy. *Journal of Environmental Management* 312 (June) : 114862. https://doi.org/10.1016/j.jenvman.2022.114862.

Zhu, Xi., Jing Liu, Andrew K.. Skidmore, Joe Premier, and Marco Heurich. 2020. A voxel matching method for effective leaf area index estimation in temperate deciduous forests from leaf-on and leaf-off airborne LiDAR data. *Remote Sensing of Environment* 240 (April) : 111696. https://doi.org/10.1016/j.rse.2020.111696.

Publisher's Note